Electronic Supplementary Material (ESI) for Chemical Communications

Selective Fluorescence Turn-on Sensor for Trace Vapor Detection of Hydrogen Peroxide

Miao Xu[§]*, Ji-Min Han*[§]*, Yaqiong Zhang, Xiaomei Yang and Ling Zang**

Department of Materials Science and Engineering, University of Utah,
36 S, Wasatch Dr., Salt Lake City, UT 84112

Supporting Information

1. Materials and general instrumentations

4-Bromo-1,8-naphthalic anhydride was purchased from TCI America and used as received. $PdCl_2$(dppf), 1,1´-Bis(diphenylphosphino)ferrocene (dppf) were purchased from Sigma-Aldrich and used as received. Bis(pinacolato)diboron acid, 9,10-diphenylanthracene(9,10-DPA) and Rhodamine 6G were purchased from Fisher Scientific and used as received. The silica gel TLC plates used as supporting matrix for incorporating C6NIB sensor molecules were purchased from EMD Chemicals Inc. (Silicycle Ultrapure Silica Gels SIL-5554-7). For comparison, the filter paper purchased from Whatman (Catalog No. 1001-150) was also used as the supporting matrix, but after boiling in deionized water for 1 hour to remove the bleaching reagents contained in the paper. All organic solvents were purchased from commercial manufacturers and used as received. Compound C6NIB is now available from Echelon Biosciences, Inc., Salt Lake City, UT, 84108.

UV-vis absorption spectra were measured on a PerkinElmer Lambda 25 spectrophotometer or Agilent Cary 100. The fluorescence spectra were measured on a PerkinElmer LS 55 spectrophotometer or Agilent Eclipse spectrophotometer. The fluorescence spectra of the solid sample (e.g., TLC plates) were recorded on an Ocean Optics USB4000 equipped with 395 nm LED light source and optical fiber (Avantes, FCR-UV200/600-2-IND) for light delivery. ^{1}H and ^{13}C NMR spectra were recorded on a Varian Unity 300 MHz Spectrometer at room temperature in appropriate deuterated solvents. All chemical shifts are reported in parts per million (ppm). MALDI TOF HRMS spectra were recorded on

UltrafleXtreme Maldi/ToF/ToF mass spectrometer (Bruker Daltonics), and the solvent used was methanol.

2. Synthesis

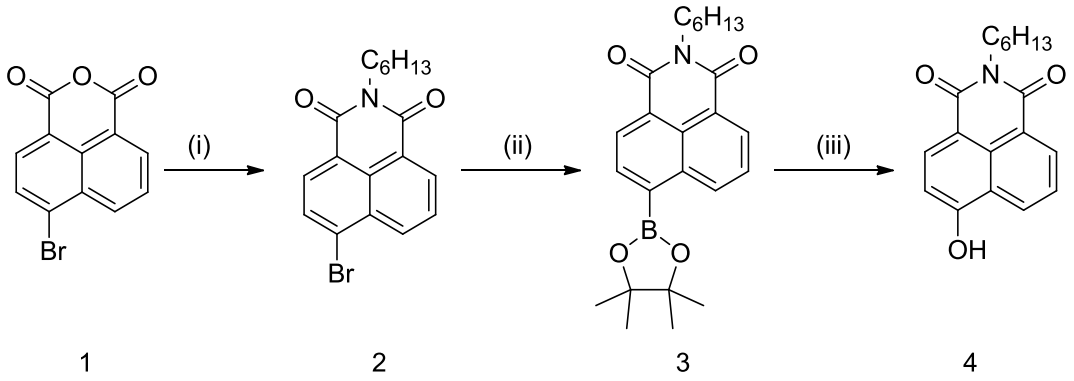

Scheme S1 The synthesis route of sensor molecule C6NIB (**3**): (i) hexylamine, triethylamine(Et_3N), ethanol, reflux, 4 h; (ii) $PdCl_2$(dppf), dppf, potassium acetate (AcOK), bis(pinacolato)diboron, N,N-Dimethylformamide (DMF), 120 °C, 3 h; (iii) DMF, 35% H_2O_2, room temperature, 3 h.

6-bromo-2-hexyl-1H-benzo[de]isoquinoline-1,3(2H)-dione (**2**): 4-Bromo-1,8-naphthalic anhydride (1 g, 3.6 mmol), hexylamine (383 mg, 3.8 mmol), triethylamine (10 mL) were added into 50 mL anhydrous ethanol and refluxed for 4 hours.[1] The reaction mixture was evaporated under reduced pressure and then purified through column chromatography on silica gel with hexane/ethyl acetate (5:1, v/v) as eluent. The product was obtained as white crystal (1.10 g, 85 %). ^{1}H NMR ($CDCl_3$, 300 MHz, ppm): δ= 8.52-8.55 (1 H, m, Ar-H), 8.39-8.43 (1 H, m, Ar-H), 8.27-8.29 (1 H, d, J = 7.8 Hz, Ar-H), 7.90-7.93 (1 H, d, J = 7.8 Hz, Ar-H), 7.71-7.76 (1 H, m, Ar-H), 4.07-4.13 (2 H, t, J = 7.2 Hz, CH_2), 1.66-1.71 (2 H, m, CH_2), 1.29-1.40 (6 H, m, CH_2), 0.84-0.8 (3 H, t, CH_3). ^{13}C NMR ($CDCl_3$, 75 MHz, ppm): δ 163.32, 163.29, 132.90, 131.76, 130.94, 130.88, 129.95, 128.65, 127.87, 122.90, 122.05, 40.51, 31.45, 27.91, 26.70, 22.49, 14.00.

2-hexyl-6-(4,4,5,5-tetramethyl-1,3,2-dioxaborolan-2-yl)-1H-benzo[de]isoquinoline-1,3(2H)-dione (**3**): **2** (360 mg, 1 mmol), anhydrous potassium acetate (588 mg, 6 mmol), bis(pinacolato)diboron (560 mg, 2.2

mmol), [$PdCl_2$ (dppf)] (73 mg, 10 mol %), and dppf (55 mg, 10 mol %) and 20 mL DMF were mixed and degassed by three freeze-pump-thaw cycles. The reaction mixture was heated at 120 °C for 3 hours. After cooling to room temperature, the reaction mixture was partitioned between water and dichloromethane. The aqueous phase was extracted with 20 mL dichloromethane for 3 times and then combined with the original dichloromethane phase. This dichloromethane solution was washed with brine twice and then washed with water, followed by drying with Na_2SO_4. After rotary evaporate under reduced pressure to remove excess solvent, the residue was purified through column chromatography on silica gel with hexane/ethyl acetate (5:1, v/v) as eluent.[2] The product was obtained as white powder (180 mg, 44 %). ^{1}H NMR ($CDCl_3$, 300 MHz, ppm): δ= 9.05-9.08 (1 H, m, Ar-H), 8.50-8.56 (2 H, m, Ar-H), 8.24-8.26 (2 H, d, J = 7.2 Hz, Ar-H), 7.71-7.76 (1 H, t, J = 7.2 Hz, Ar-H), 4.11-4.16 (2 H, t, J = 7.2 Hz, CH_2), 1.71 (2 H, m, CH_2), 1.30-1.35 (6 H, m, CH_2), 0.85-0.90 (3 H, t, CH_3). ^{13}C NMR ($CDCl_3$, 75 MHz, ppm): δ 164.16, 164.14, 135.66, 135.11, 134.77, 130.70, 129.59, 127.69, 126.95, 124.62, 122.51, 84.48, 40.43, 31.50, 27.96, 26.74, 24.91, 22.50. MALDI TOF-HRMS *m/z*: Calcd for $C_{24}H_{30}BNO_4$: 407.2268, Found: 408.2367 $[M+H]^+$.

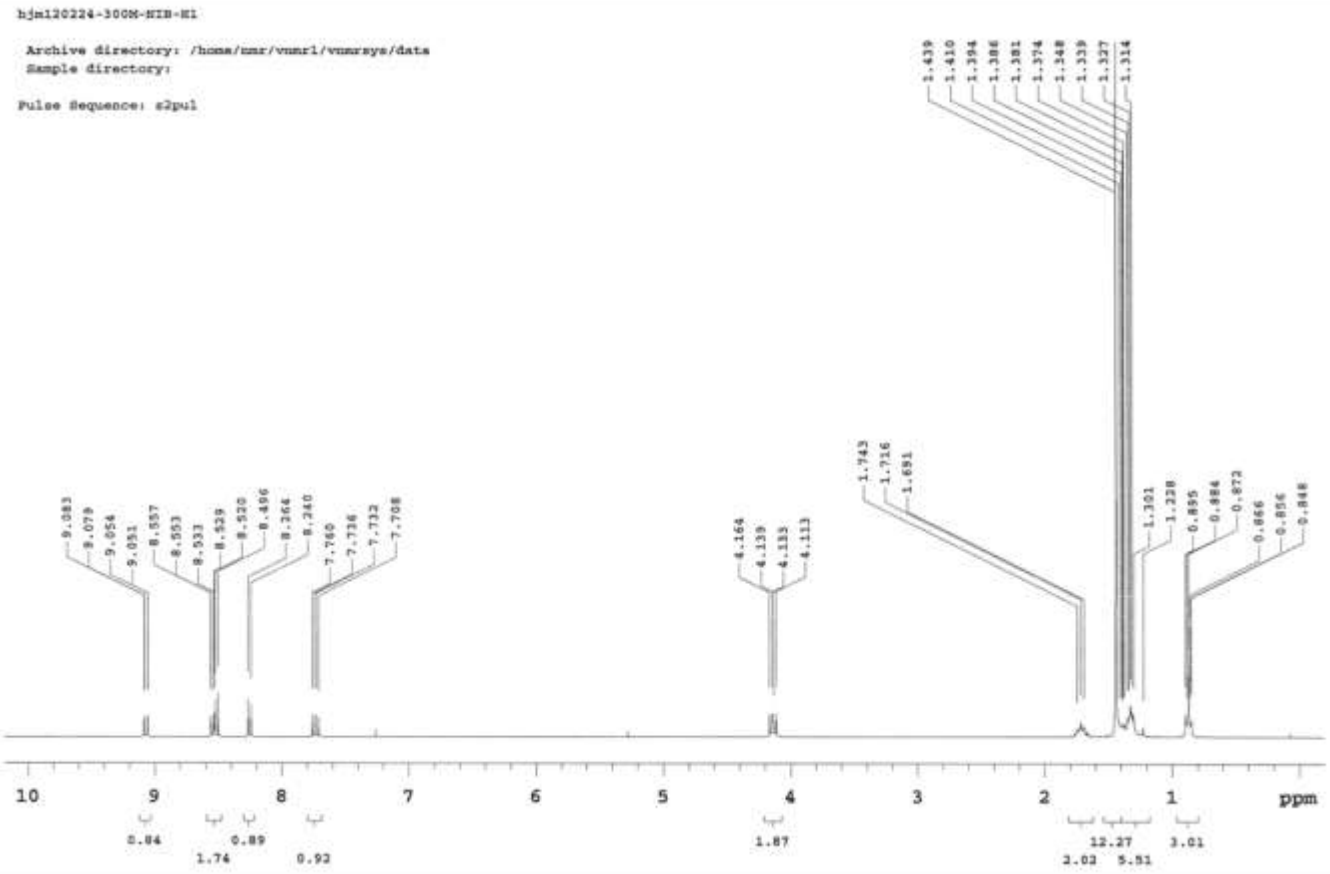
bjm120224-300M-NIB-H1
Archive directory: /home/nmr/vnmrl/vnmrsys/data
Sample directory:
Pulse Sequence: s2pul
ppm
0.84
1.74
0.89
0.92
1.87
3.02
12.27
5.51
3.01

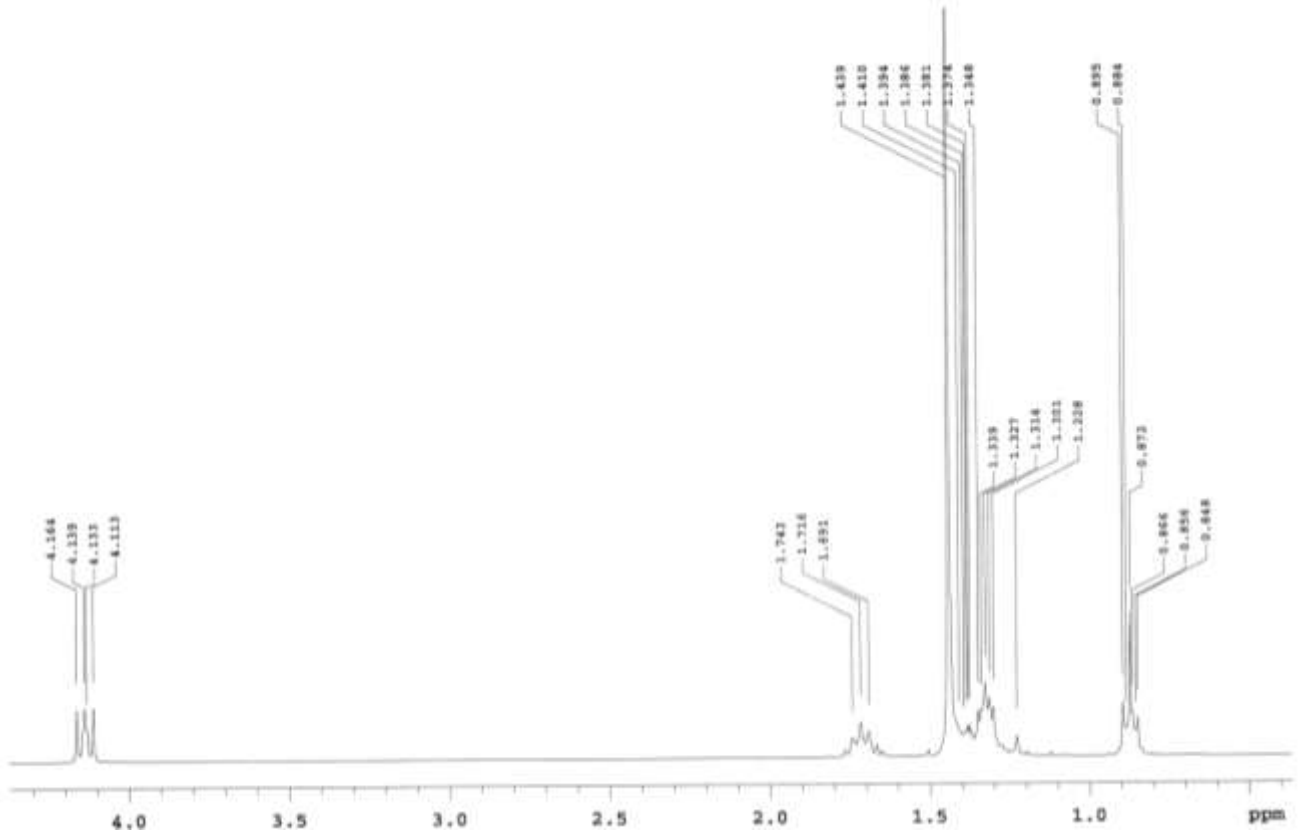
4.0
3.5
3.0
2.5
2.0
1.5
1.0
ppm

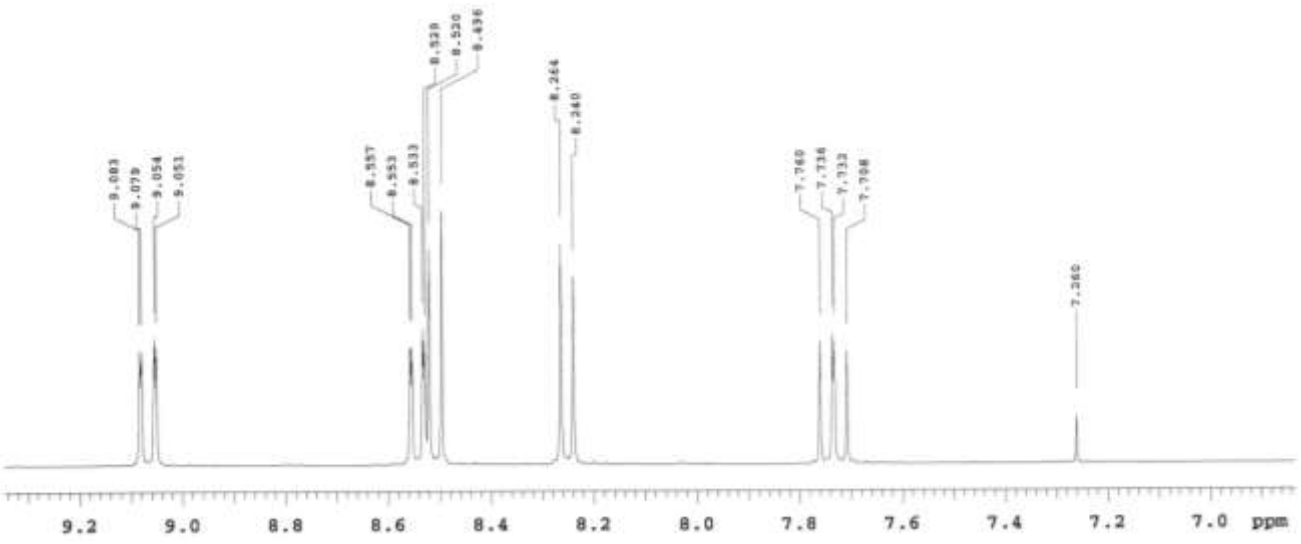

^{1}H NMR spectrum of C6NIB

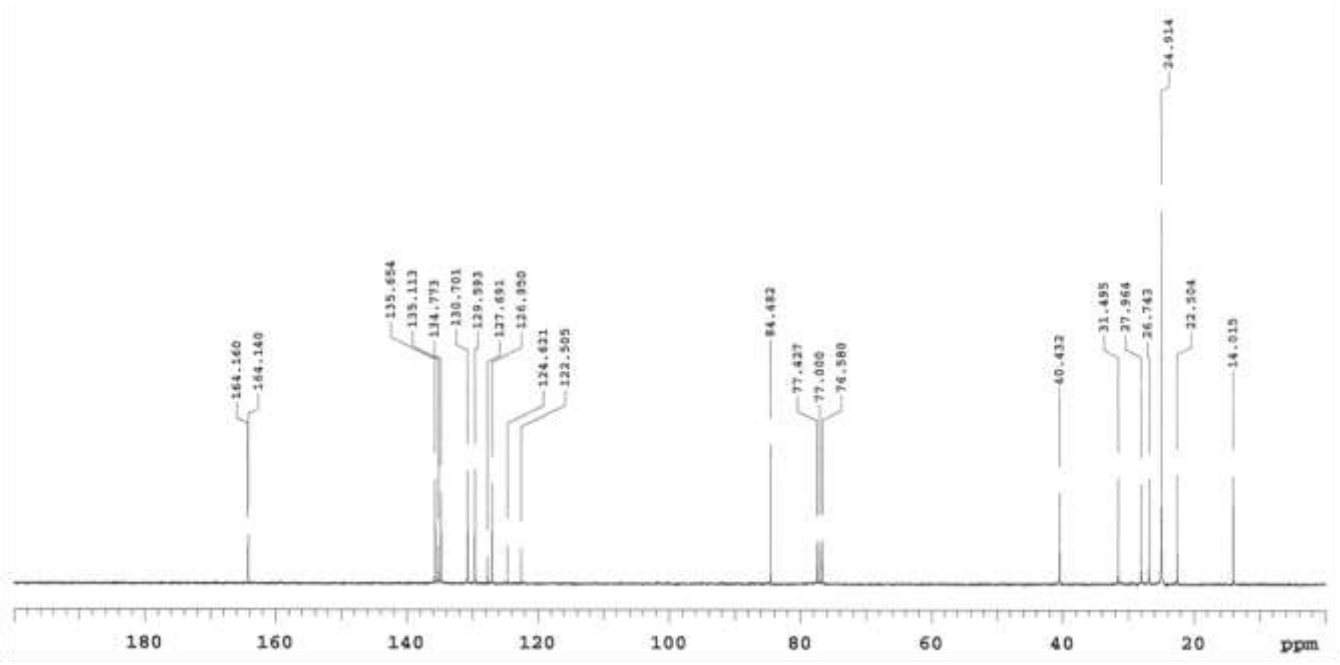

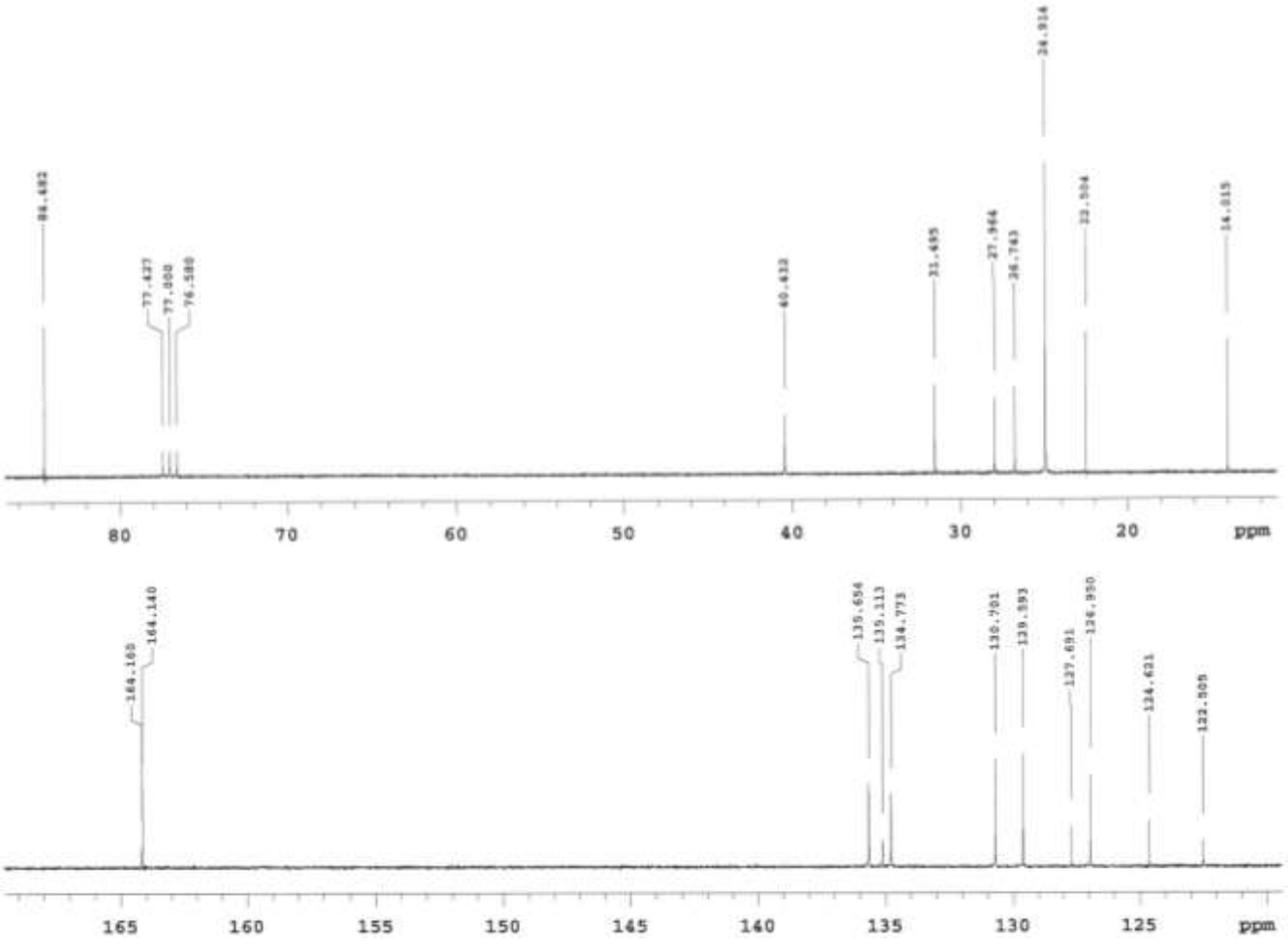

^{13}C NMR spectrum of C6NIB

2-hexyl-6-hydroxy-1H-benzo[de]isoquinoline-1,3(2H)-dione (**4**) : To a solution of **3** (81 mg, 0.20 mmol) in 10 mL DMF, 2 mL H_2O_2 (35 wt%) was added, followed by stirring at room temperature for 3 h. The reaction solution was then diluted with ethyl acetate, extracted with 1 M HCl and brine, and dried over Na_2SO_4. After removal of solvent, the crude product was purified by flash chromatography (methylene chloride/methanol = 150:1) on silica gel to give 15 mg yellow product **4**, yield 51%, ^{1}H NMR (CD_3CN, 300 MHz, ppm): δ = 8.49-8.54 (2 H, m, Ar-H), 8.36-8.39 (2 H, d, J = 8.1 Hz, Ar-H), 7.69-7.75 (1 H, m, Ar-H), 7.11-7.14 (1 H, d, J = 8.1 Hz, Ar-H), 4.04-4.09 (2 H, m, CH_2), 1.66-1.68 (2 H, m, CH_2), 1.31-1.41 (6 H, m, CH_2), 0.86-0.91 (3 H, t, CH_3). ^{13}C NMR (DMSO-d_6, 75 MHz, ppm): δ 163.63, 162.97, 160.25, 133.54, 131.11, 129.15, 128.87, 125.59, 122.36, 121.79, 112.58, 109.95, 39.36,

30.97, 27.50, 26.21, 21.98, 13.91. MALDI TOF-HRMS m/z: Calcd for C18H19NO3: 297.1365, Found: 298.1430 $[M+H]^+$.

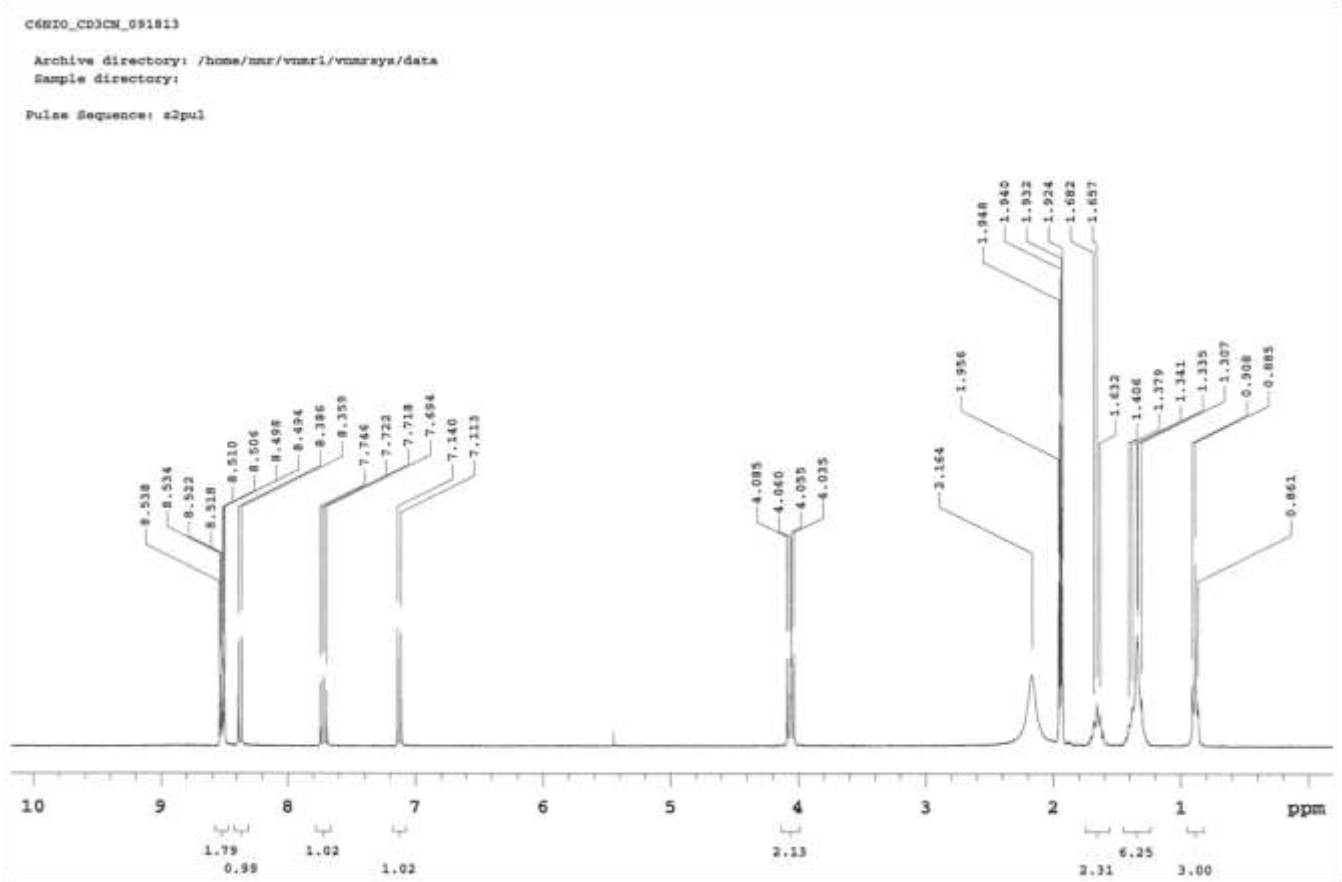

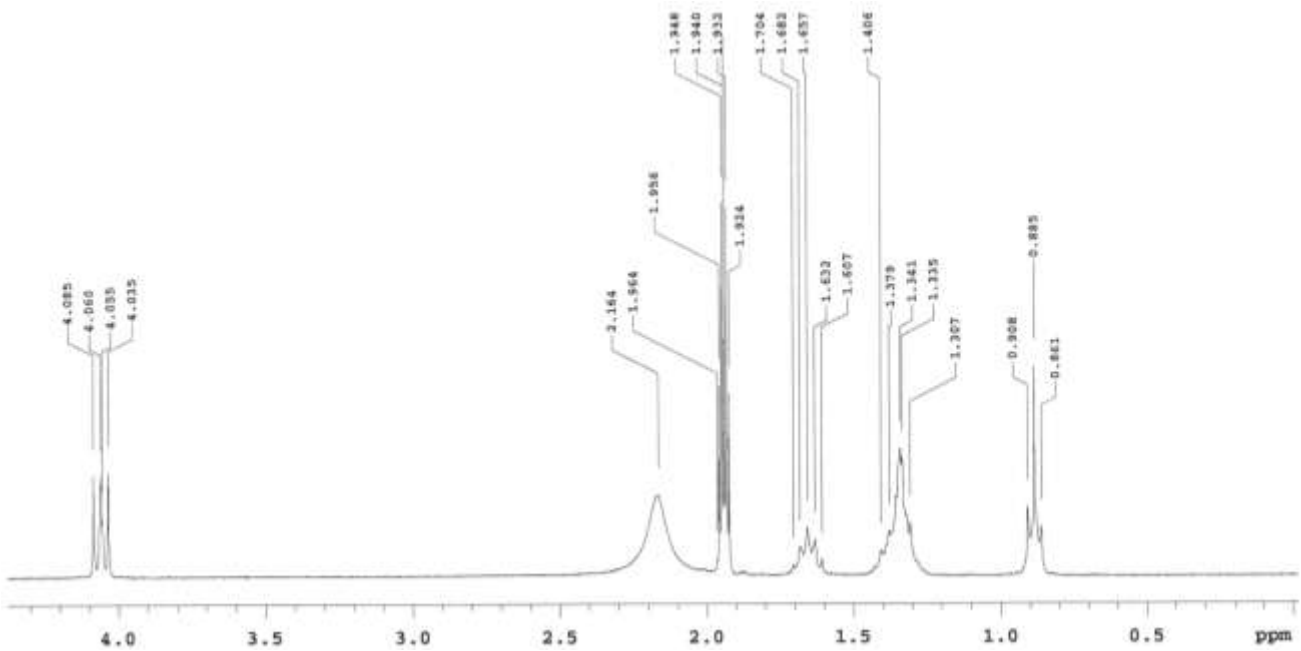

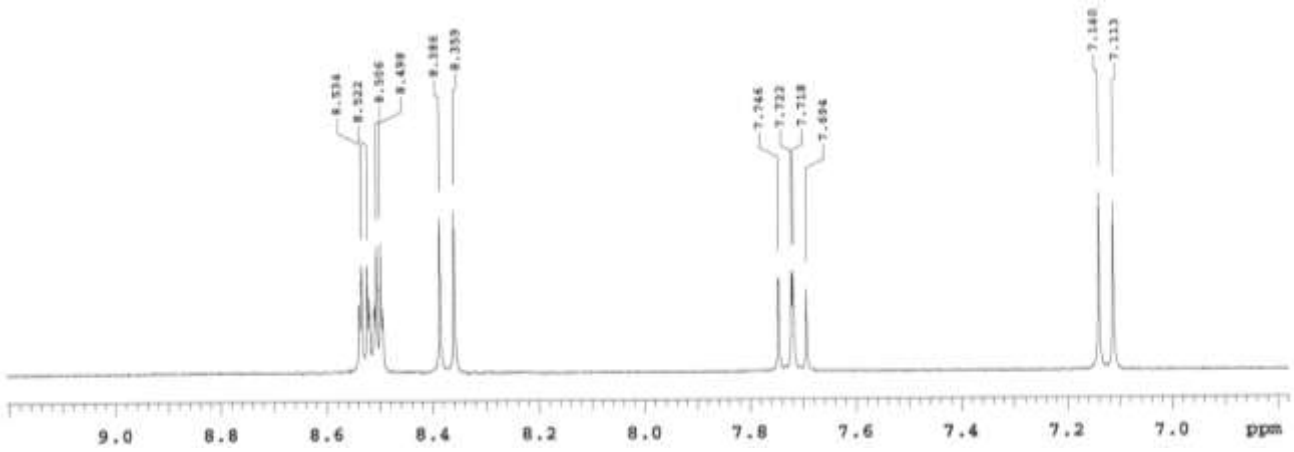

^{1}H NMR spectrum of C6NIO

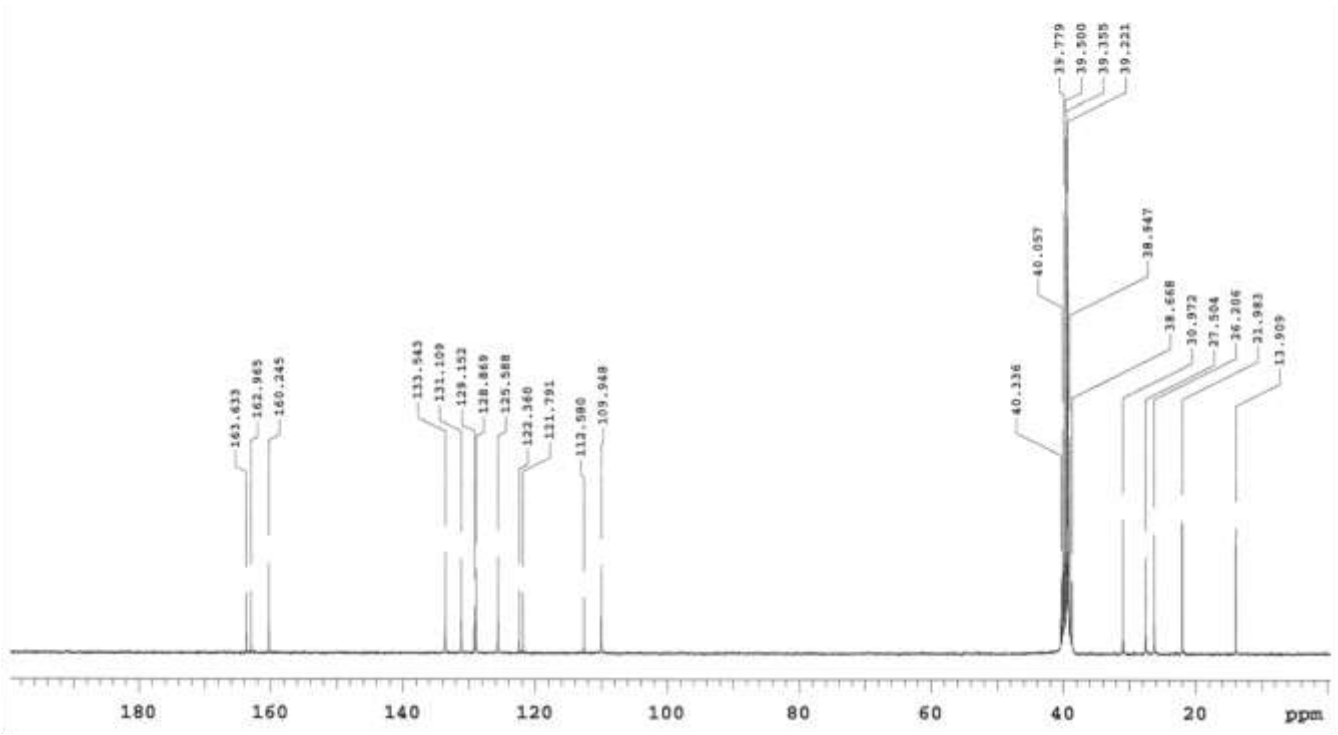

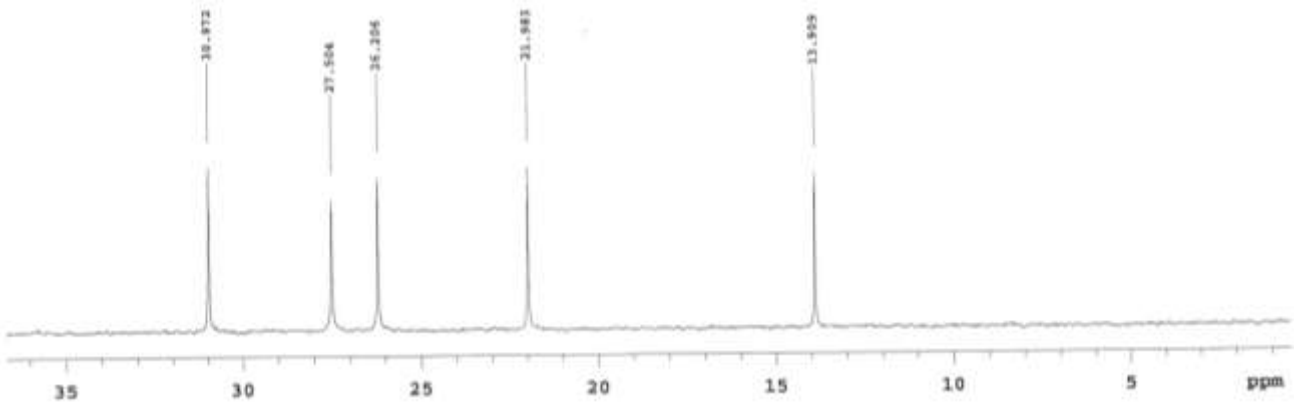

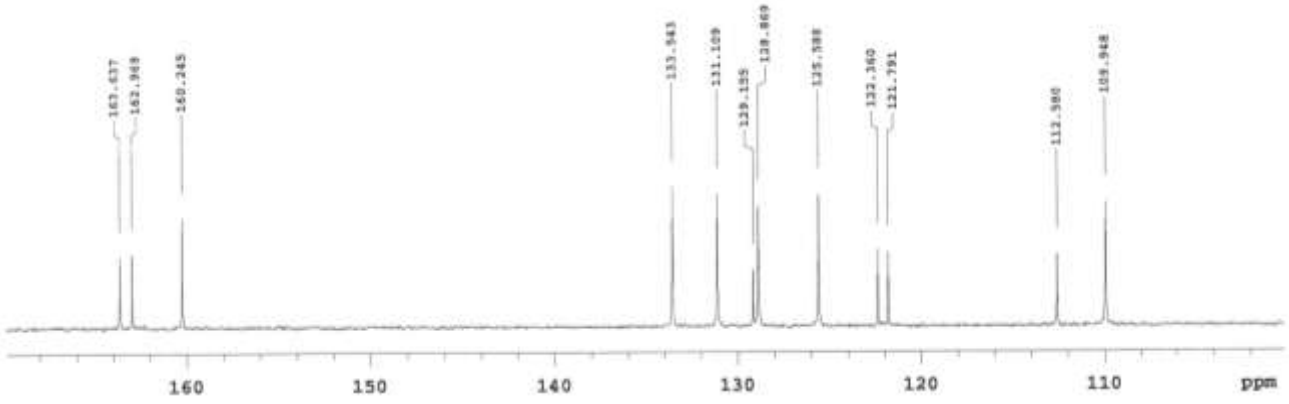

^{13}C NMR spectrum of C6NIO

3. Other experimental details

Dispersion of sensor molecules in silica gel TLC plate and filter paper matrix. 50 μL ethanol solution of C6NIB at different concentrations (also containing appropriate concentrations of TBAH as detailed below) was drop-cast uniformly onto a 1.5×1.5 cm^2 silica gel TLC plate, followed by drying at room temperature in vacuum for 1 hour. To adjust the molar amount of C6NIB loading (as indicated in Fig. S7), various concentrations of C6NIB in ethanol were prepared and used: 0.1, 0.01 and 0.001 mol/L. Uniform dispersion of C6NIB sensor molecules within the TLC plate is indicated by the uniform emission density shown in the emission photography of the plate after exposure to the H_2O_2 vapor (Fig. 1d). The same dispersion method was also used for dispersing the sensor molecules into Al_2O_3 TLC plate and filter paper, which were used for comparative sensor investigation as shown in Fig. S4.

Fluorescence quantum yield measurement. As shown in Fig. S1, molecule C6NIB is only weakly fluorescent in the UV region (λ_{max} at 392 nm) mainly due to the π–π* transition of naphthalimide backbone, while C6NIO is strongly fluorescent in the longer wavelength region (λ_{max} at 550 nm) due to the charge transfer transition. The quantum yields (Φ) of C6NIB and C6NIO were determined by a single-point measurement with a standard sample of known quantum yield.[3] 9,10-diphenylanthracene(9,10-DPA) (Φ=0.95 in cyclohexane)[4] and Rhodamine 6G (Φ=0.94 in ethanol)[5]

were chosen as standard samples for C6NIB and C6NIO, respectively. The excitation wavelengths were selected as 340 nm and 480 nm for 9,10-DPA/C6NIB and Rhodamine 6G/C6NIO, respectively. The quantum yields of C6NIB and C6NIO in ethanol (in the presence of 100 fold TBAH) were determined as 0.069 and 0.254, respectively. The quantum yield of C6NIB in ethanol (in the presence of 100 fold TBAH) is only 0.006.

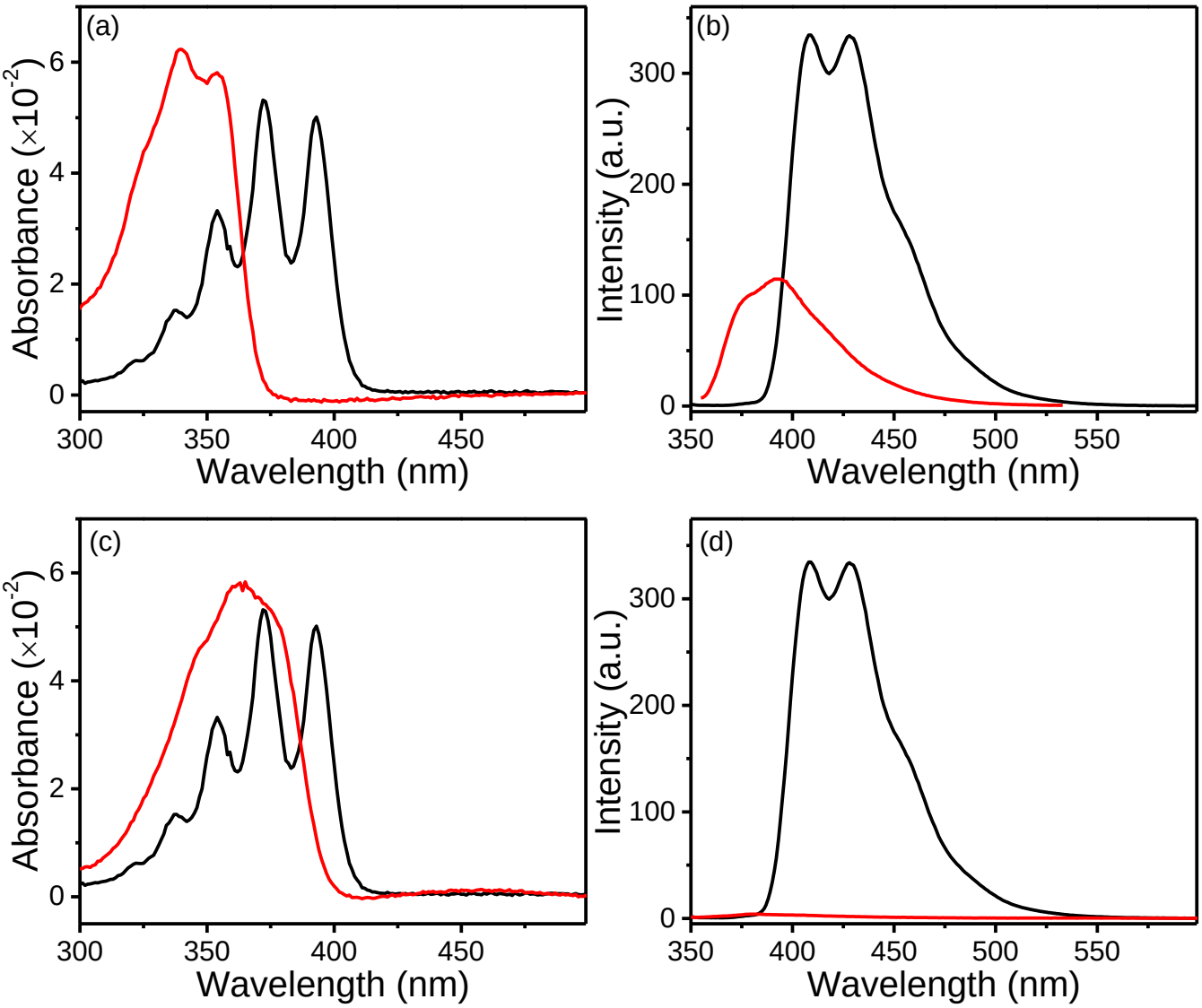

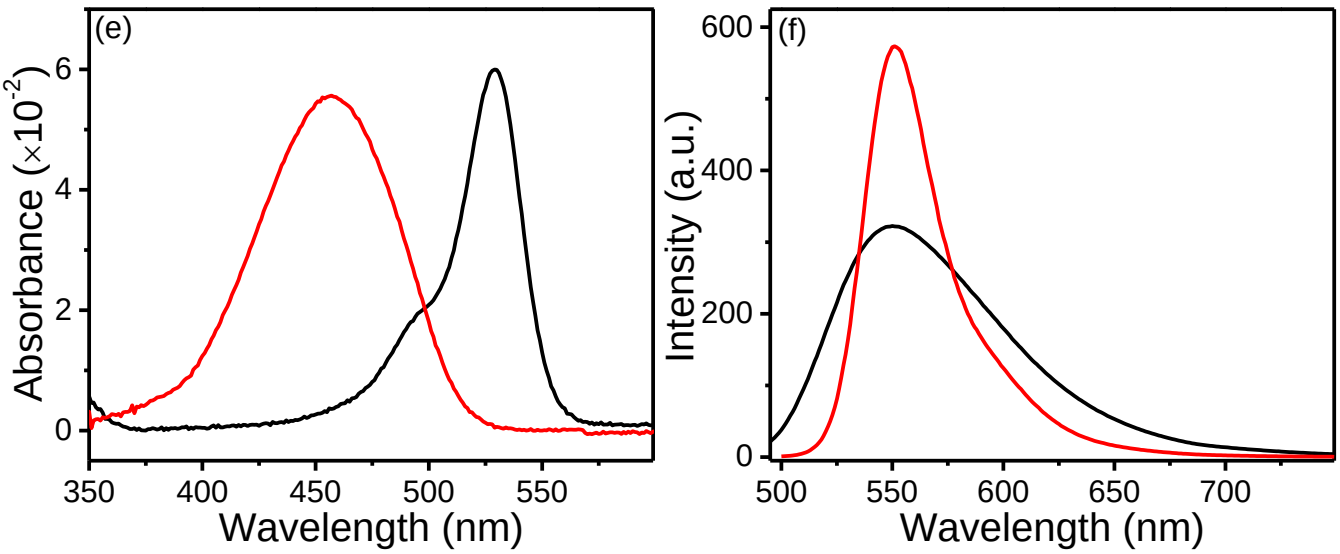

Fig. S1 Absorption and fluorescence spectra of C6NIB, C6NIO, and the corresponding standard fluorophores used for measuring the quantum yields: (a,b) C6NIB in ethanol (red) and 9,10-DAP in cyclohexane (black); (c,d) C6NIB with 100 molar fold TBAH in ethanol (red) and 9,10-DAP in cyclohexane (black); (e,f) C6NIO with 100 molar fold TBAH in ethanol (red) and Rhodamine 6G in ethanol (black).

Sensor stability test on silica gel TLC plate. The C6NIB dispersed TLC plate sample was prepared according to the method description above, and fluorescence spectra were measured at different time intervals after preparation (Fig. S2), which did not show significant change in fluorescence spectra or intensity within the experimental investigation period. The same TLC plate was then exposed to 225 ppm H_2O_2 vapor for 5 minutes, followed by measurement of the fluorescence spectrum.

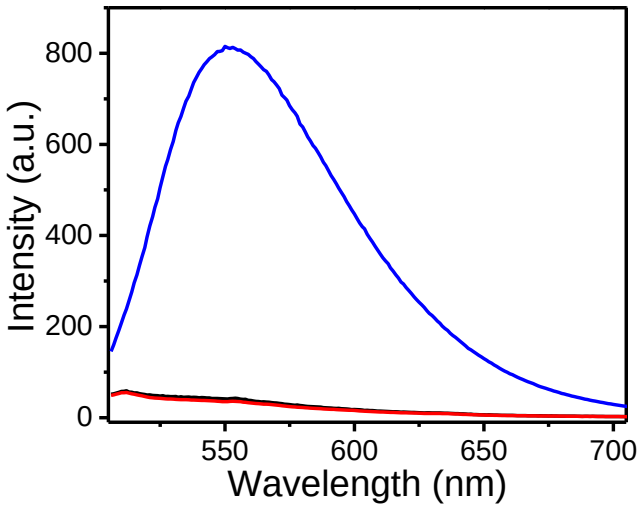

Fig. S2 The fluorescence spectra of C6NIB dispersed in a 1.5×1.5 cm^2 silica gel TLC plate (containing 0.5 μmol C6NIB and 5 μmol TBAH): freshly prepared TLC plate (black), after 7 days (red), and after exposure to 225 ppm H_2O_2 vapor for 5 min (blue).

Time course of sensor response in solid matrices. To find the optimal concentration of TBAH (or molar ratio TBAH/C6NIB) that would give the fasted sensor reaction, i.e., the H_2O_2 mediated oxidation of C6NIB to C6NIO (as shown in Fig. 1), we measured the time course of the fluorescence intensity change at 553 nm for the sensor molecules dispersed in silica gel TLC plates The optimization experiments were performed for the sensor molecules dispersed in silica gel TLC plates as shown in Fig. S3, where the time course of the fluorescence intensity change was measured at 553 nm for C6NIB dispersed in a 1.5×1.5 cm^2 silica gel TLC plate (containing 0.5 μmol C6NIB) upon exposure to H_2O_2 vapor fixed at 225 ppm. Four series of measurements were performed over the TLC plates containing the same molar amount of C6NIB, but different amounts of TBAH, i.e., at molar ratios of TBAH/C6NIB: 1, 10, 50 and 100. The testing experiment was performed by hanging the loaded TLC plate in the saturated vapor of H_2O_2 (225 ppm) above 10 mL of 35 wt % H_2O_2 solution sealed in a 50 mL jar. The fluorescence emission evolved at different time intervals was measured by Ocean Optics USB4000 spectrophotometer. As shown in Fig. S3, the fluorescence intensity increased the fastest and reached the highest intensity value at TBAH/C6NIB ratio of 10, which was determined as the optimal

molar ratio for fabricating the sensor composite. The slower sensor response observed at higher TBAH/C6NIB ratio (e.g., 50, 100) is likely due to that the excessive TBAH blocks the porous structure silica gel, thus weakening the gas intake of H_2O_2 vapor.

For the measurements performed under varying vapor concentrations of H_2O_2 (shown Fig. S6 and Fig. 3), the testing experiment was performed by hanging the loaded TLC plate in the saturated vapor of H_2O_2 generated in a 26.5 L container, where approximately 1 L of H_2O_2 solution (diluted down to various concentrations) was put in a and sealed for 12 hours to reach the equilibrium vapor pressure. The equilibrium vapor pressure corresponding to a specific diluted concentration of H_2O_2 solution was deduced from the literature.[6] In the container, continuous vapor stream was produced by a mini fan (Radio Shack, 40mm, 12VDC, 6500RPM), and the sensor loaded TLC plate was placed against the vapor stream (distanced from the fan by 0.5 cm), and about 20 cm above the solution surface. After exposure to the vapor for different time intervals, the TLC plate was taken out for fluorescence measurement. In this study, various diluted concentrations of H_2O_2 solution were obtained by diluting the commercial 35 wt % solution with pure water 100, 500, 1000, 2000, and 10000 times, which produce saturated (equilibrium) vapor pressures of H_2O_2 of 1000, 200, 100, 50 and 10 ppb, respectively.[6]

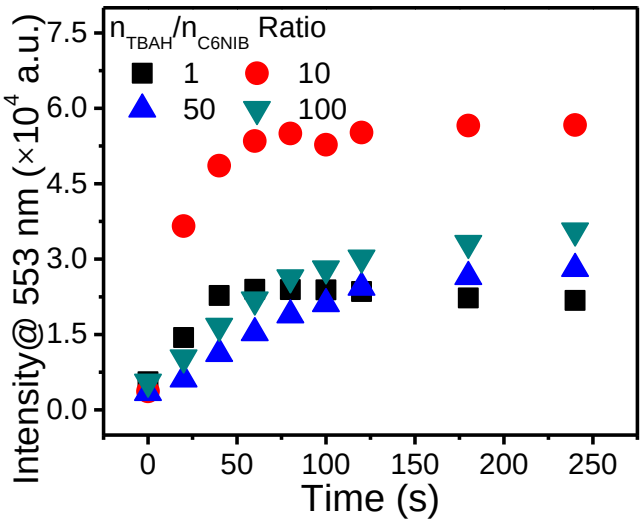

Fig. S3 Time course of the fluorescence intensity change measured at 553 nm for C6NIB dispersed in a 1.5×1.5 cm^2 silica gel TLC plate (containing 0.5 μmol C6NIB) upon exposure to 225 ppm H_2O_2 vapor. Shown in the Fig. S3 are four series of measurements performed over the TLC plates containing the same molar amount of C6NIB, but different amounts of TBAH, i.e., at molar ratios of TBAH/C6NIB: 1, 10, 50 and 100.

Comparison of sensor response between different supporting matrices. The sensor testing as shown in Fig. S3 was also performed over the sensor molecules dispersed in alumina TLC plate and filter paper. Although these two materials also possess large porosity and surface area, the sensor efficiency (regarding both response speed and fluorescence turn-on ratio at saturate stage) was found significantly lower than that observed for silica gel TLC plate. This is likely due to the hydrophilic surface of silica gel that is more conducive for the homogeneous dispersion of TBAH/C6NIB as discussed in the main context of this manuscript.

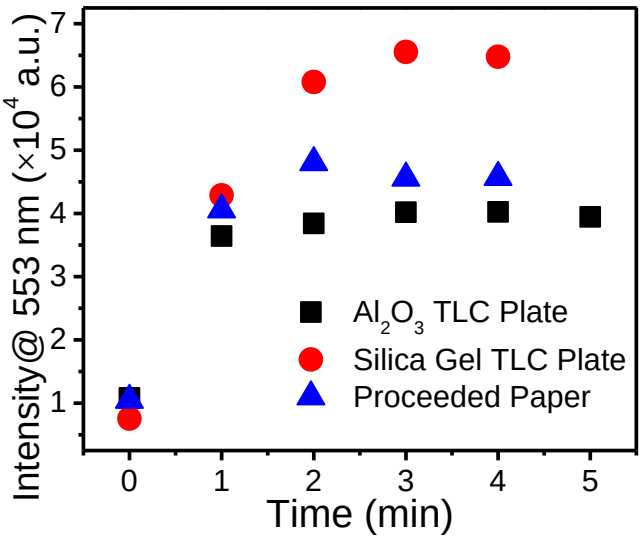

Fig. S4 Time course of the fluorescence intensity change measured at 553 nm for C6NIB dispersed in different supporting materials (Al_2O_3 TLC plate, silica gel TLC plate, filter paper), all in the area size of 1.5×1.5 cm^2, and containing 0.5 μmol C6NIB and 5 μmol TBAH.

Comparison of sensor response with different bases. The sensor testing as shown in Fig. S5 was performed over the sensor molecules dispersed in silica TLC plate to compare the different sensing response towards H_2O_2 vapor when using different bases. Compared to NaOH (which is a common base used in deboronation reaction), TBAH produced much higher fluorescence intensity (implying much more efficient sensor conversion) under the same reaction conditions.

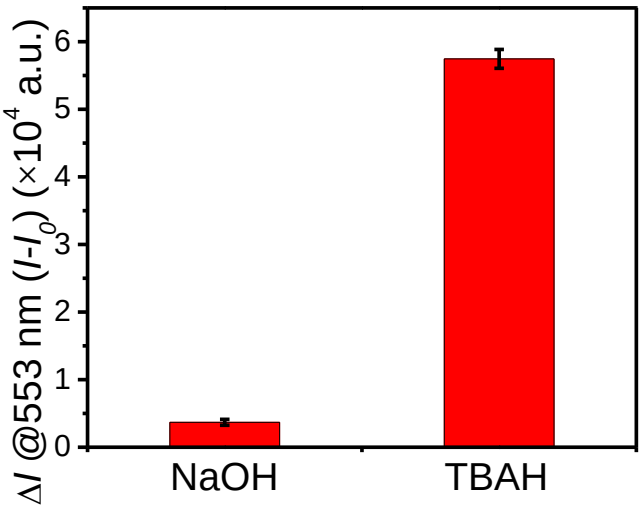

Fig. S5 The increase in fluorescence intensity observed for the TLC plate samples treated with the same sensor but different bases (NaOH and TBAH); the fluorescence was monitored at 553 nm after exposure

to 225 ppm H_2O_2 vapor for 5 min. The TLC plates were in the size of 1.5×1.5 cm^2, and containing 0.5 μmol C6NIB and 5 μmol base. The error bars are based on the standard deviations of the data.

Selectivity test. The sensor loaded TLC plate tested in Fig. 1 were exposed to the saturated vapor of various common solvents such as ethanol (89,000 ppm), methanol (131,000 ppm), acetone (260,000 ppm), THF (173,000 ppm), hexane (130,000 ppm), toluene (26,000 ppm), ethyl acetate (100,000 ppm), chloroform (140,000 ppm), to validate the selectivity of the sensor molecule. The increase in fluorescence intensity was measured at 553 nm over C6NIB loaded silica gel TLC plate (the same component as used in Fig. 1d) after 5 min exposure to 225 ppm H_2O_2 vapor, in comparison to that upon exposure to the saturated vapor of the common solvents. Although the vapor pressures of the reference solvents are about three orders of magnitude higher than that of H_2O_2, our experiments did not demonstrate any significant fluorescence emission evolution even after extensive exposure to these highly concentrated solvents vapor. This clearly proves the high selectivity of the sensor molecule C6NIB for detection of H_2O_2. The error bars shown in Fig. 1b are based on the standard deviations of the data.

Fitting of the data presented in the inset of Fig. S6. The data presented in the inset of Fig. S6 can be fitted following the reaction kinetics equation,[7]

$$\Delta I = K'(1 - e^{-Kt}) \quad (1)$$

where ΔI is the increase in fluorescence intensity measured at 553 nm, K and K' are constants with K related to the surface reaction rate of C6NIB with H_2O_2, the given vapor pressure of H_2O_2 and the total load of C6NIB, and K' is referred to as the ratio of the fluorescence intensity to the molar fraction of C6NIO (with respect to the total starting amount of C6NIB). Derivation of this equation is based on the surface reaction kinetics, i.e. the rate of producing C6NIO is proportional to the surface density (or molar fraction) of unreacted C6NIB.

The fitting gives K'=28176.33, K=0.01193, with a R^2= 0.9941, then the reaction time can be projected at a given ΔI

$$t = -\frac{\ln(\frac{-\Delta I + K'}{K'})}{K}$$

The standard derivation (δ) of the emission intensity measurement shown in Fig. 3 was about 96 (a.u.). The threshold of detectable emission can be set at an intensity level three times of the standard derivation (3δ), which is 288. Then, the corresponding sensor response time (t) can be determined as ca. 0.86 sec.

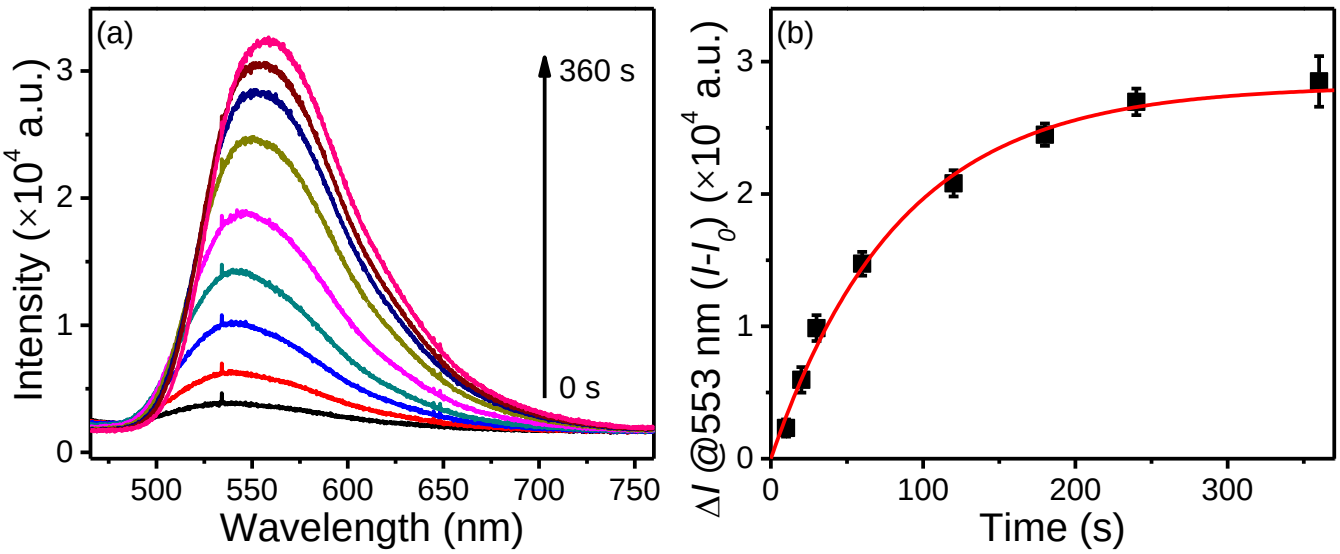

Fig. S6 (a) The fluorescence spectra of C6NIB dispersed in a 1.5×1.5 cm^2 silica gel TLC plate (containing 0.5 μmol C6NIB and 5 μmol TBAH) recorded at various time intervals after exposure to 1 ppm H_2O_2 vapor. (b) The emission intensity increase ΔI measured at 553 nm as a function of exposure time, for which the data points are fitted following a first order surface reaction between C6NIB and H_2O_2. The error bars are based on the standard derivations of the intensities as measured.

Fitting of the data presented in the inset of Fig. 3b Assuming a quasi equilibrium was reached within 5 min exposure (as implied from the result in Fig. S6) to H_2O_2 vapor, the results shown Fig. 3b should follow the Langmuir adsorption model. First, the surface adsorption of H_2O_2 (i.e., the reacted fraction of sensor molecules, X) is related to the vapor pressure of H_2O_2 as described by the Langmuir Equation,

$$X = \frac{b \cdot [H_2O_2]}{1 + b \cdot [H_2O_2]}$$

Where b is a constant, $[H_2O_2]$ is the vapor pressure (concentration) of H_2O_2.

The fluorescence emission intensity is proportional to the concentration of sensor molecules converted. Then, we have

$$\Delta I = \frac{a \cdot b \cdot [H_2O_2]}{1 + b \cdot [H_2O_2]}$$

Where a is a proportional constant.

The fitting gives a=36986.6, b=0.0027 with a R^2= 0.9813.

The standard derivation of the emission intensity measurement shown in Fig. 3 was about 96 (a.u.). The threshold of detectable emission can be set at an intensity level three times of the standard derivation, that's ΔI = 288. Then, the corresponding detection limit can be determined by using the above equation and substituting ΔI with 288. This gives a detection limit of H_2O_2 vapor at 2.9 ppb.

Absorption (extinction) spectral measurement. Due to the nontransparency of the TLC plate, the absorption spectra of the sensors dispersed in this medium had to be measured in reflection mode, which can then be converted into extinction spectral data (in analogy to light absorption). The reflection spectra were recorded on a PerkinElmer Lambda 650R spectrophotometer with a build-in universal reflection accessory. The spectra were collected with unpolarized light incident at ~45° with respect to the surface and integrated for 0.1 s and at a resolution of 1 nm. The spectra collected were converted and shown as extinction measured as $-\log(R/R_0)$, where R is the reflectance of the loaded sample substrate and R_0 is the reflectance of the unload TLC plate substrate.[8]

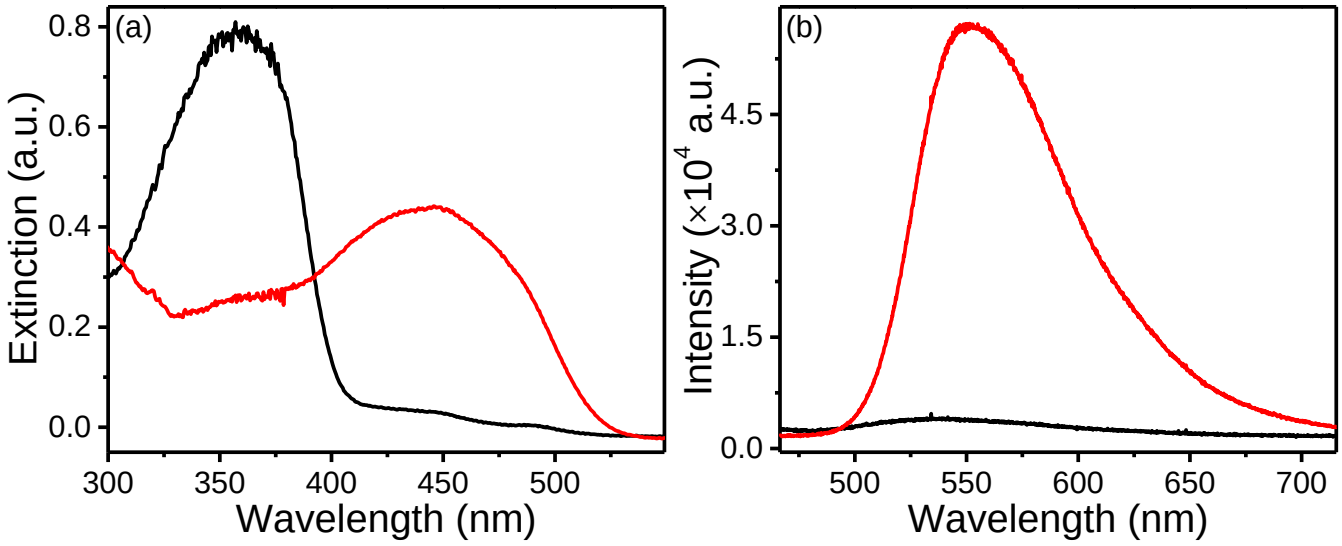

Fig. S7 (a) Extinction (converted from reflection spectrum) and (b) fluorescence spectra of C6NIB dispersed in a 1.5×1.5 cm^2 silica gel TLC plate (containing 0.5 μmol C6NIB and 5 μmol TBAH) before (black) and after (red) exposure to 225 ppm H_2O_2 vapor for 5 min.

Absorption and fluorescence spectra of C6NIO solution and film. To study in detail the spectral property (the ICT transition band) of C6NIO and the dependence on deprotonation of the phenol group, the UV-vis absorption and fluorescent spectra of C6NIO in ethanol solution were measured with addition of TBAH at different molar ratios of TBAH/ C6NIO, ranging from 1 to 100. As shown in Fig. S8a, the ICT absorption band increased dramatically with the addition of TBAH and reached its maximum at molar ratio of TBAH/ C6NIO of 10. This increase in ICT band is due to the deprotonation process, transforming phenol group of C6NIO to phenolate. The corresponding ICT emission band of C6NIO showed a similar change upon addition of TBAH, also reaching its maximal intensity at molar ratio of TBAH/ C6NIO of 10 (Fig. S8b).

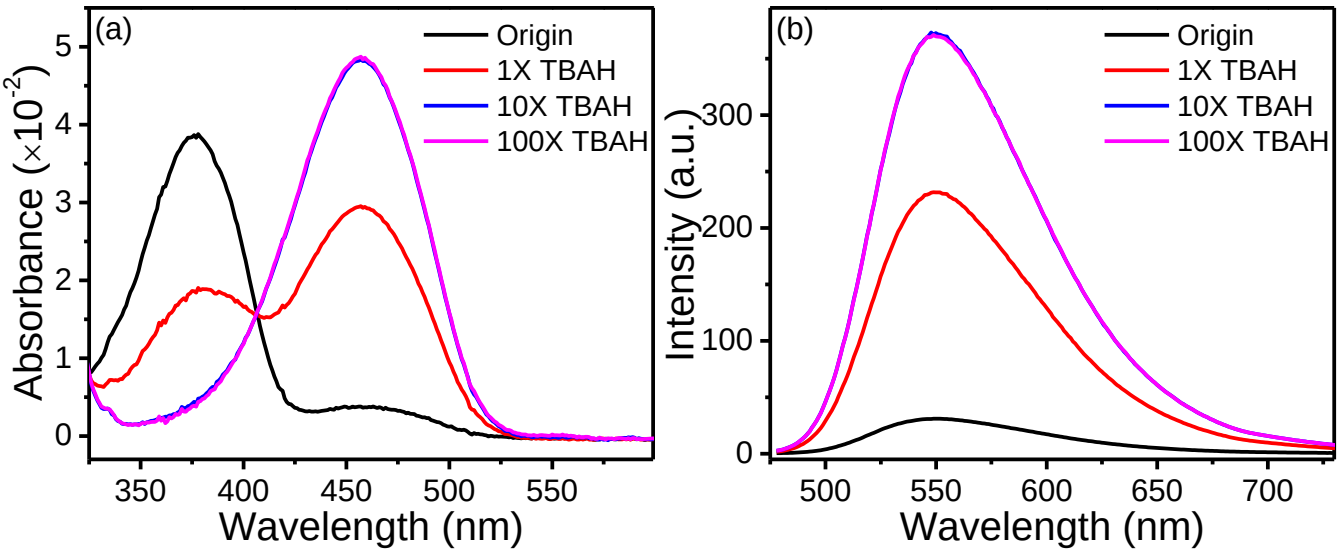

Fig. S8 (a) Absorption and (b) fluorescence spectra of an ethanol solution of C6NIO (black, 5×10^{-6} mol/L) with addition of different amount of TBAH (red, 5×10^{-6} mol/L; blue, 5×10^{-5} mol/L; purple, 5×10^{-4} mol/L), λ_{ex}=458 nm.

1. J. Wu, T. Yi, T. Shu, M. Yu, Z. Zhou, M. Xu, Y. Zhou, H. Zhang, J. Han, F. Li and C. Huang, *Angew. Chem. Int. Ed.*, 2008, **47**, 1063-1067.
2. F. Thiemann, T. Piehler, D. Haase, W. Saak and A. Lützen, *Eur. J. Org. Chem.*, 2005, **2005**, 1991-2001.
3. J. R. Lakowicz, *Principles of Fluorescence Spectroscopy*, Kluwer Academic/Plenum Publishers, New York, 1999.
4. M. Mardelli and J. Olmsted Iii, *Journal of Photochemistry*, 1977, **7**, 277-285.
5. M. Fischer and J. Georges, *Chem. Phys. Lett.*, 1996, **260**, 115-118.
6. S. L. Manatt and M. R. R. Manatt, *Chem. Eur. J.*, 2004, **10**, 6540-6557.
7. M. Xu, B. R. Bunes and L. Zang, *ACS Appl. Mater. Interfaces*, 2011, **3**, 642-647.
8. J. D. Driskell, R. J. Lipert and M. D. Porter, *J. Phys. Chem. B*, 2006, **110**, 17444-17451.